Ann Med Res

Current issue list available at AnnMedRes

Annals of Medical Research

journal page: www.annalsmedres.org

Identification of PDE10A related proteins via proteomic analysis

Mustafa Caglar Beker[a,*], Hayriye Ecem Yelkenci[b], Berrak Caglayan[c], Ertugrul Kilic[a]

[a] *Istanbul Medipol University, School of Medicine, Department of Physiology, Istanbul, Türkiye*
[b] *Istanbul Medipol University, Research Institute for Health Sciences and Technologies (SABITA), Regenerative and Restorative Medicine Research Center (REMER), Istanbul, Türkiye*
[c] *Istanbul Medipol University, International School of Medicine, Department of Medical Genetics, Istanbul, Türkiye*

ARTICLE INFO

Keywords:
Liquid chromatography-tandem mass spectrometry
Phosphodiesterase 10A
Proteomics
TAK-063

Received: May 06, 2022
Accepted: Jul 26, 2022
Available Online: 26.08.2022

DOI:
10.5455/annalsmedres.2022.05.153

Abstract

Aim: Phosphodiesterase 10A (PDE10A) regulates the expression of secondary messengers of cyclic adenosine monophosphate and cyclic guanosine monophosphate, which control several intracellular signaling pathways. Recently, deactivation of PDE10A has been a notable target for the treatment of neurodegenerative diseases. Herein, we identified the effects of PDE10A inhibition on protein profile using TAK-063 under physiological conditions in mice.

Materials and Methods: In this study, 8-12 weeks old male C57BL6/J mice were divided into vehicle or 3 mg/kg TAK-063 groups. Thirty minutes after oral delivery of vehicle or TAK-063, animals were sacrificed and liquid chromatography-mass spectrometry/mass spectrometry (LC-MS/MS) mediated proteomic analyses were performed from tissue samples taken from the striatum region of mice. After the LC-MS/MS analysis, identified proteins were classified based on biological activity, molecular function, and signal transduction pathways using PANTHER (protein annotation through evolutionary relationship, http://www.pantherdb.org/) program.

Results: As a result of proteomic analyses, 1873 different proteins were identified. Sixty-one different proteins changed significantly depending on the administration of TAK-063. According to PANTHER classification, a significant part of the identified proteins found to be in the metabolite interconversion enzyme, transporter, and protein modifying enzyme category. The molecular function classification includes the catalytic activity, transporter activity, and binding functions. The signal transduction pathway analysis demonstrated that PDE10A affects ATP synthesis, FGF signaling, EGF receptor signaling, Huntington's Disease, Parkinson's Disease, pyrimidine metabolism, and ubiquitin-proteasome signal transduction pathways.

Conclusion: TAK-063 mediated PDE10 deactivation is an essential target in the mechanism of energy metabolism and neurodegenerative diseases.

Introduction

The phosphodiesterase (PDE) superfamily contains 11 different PDE proteins (PDE1 through PDE11) with diverse enzyme and substrate specificities. Also, they differ in the protein expression profiles in human tissue. Phosphodiesterases (PDEs) regulate cyclic nucleotide levels in the central nervous system (CNS) and peripheral tissues. PDEs hydrolyze the cyclic adenosine monophosphate (cAMP) and cyclic guanosine monophosphate (cGMP) to 5'-adenylic acid (5'-AMP) and 5'-guanidylic acid (5'-GMP), respectively. Secondary messengers, cAMP and cGMP, are essential regulators of many intracellular signaling mechanisms, including apoptosis immune system and cell proliferation. Recent studies indicated that PDEs play a crucial role in the neuronal function, synaptic plasticity, homeostasis, cognition, and anxiety. Therefore, the PDE superfamily has become an important therapeutic target in CNS injuries [1-3].

PDE10A is a double substrate enzyme that regulates the inactivation of cAMP and cGMP to 5'-AMP and 5'-GMP, respectively. It has a higher affinity for cAMP compared to the affinity for cGMP [4]. PDE10A is highly available and scattered in the striatum region, which is the central input of the basal ganglia, and is closely related to cognitive and motor functions [5, 6]. It regulates the du-

*Corresponding author:
Email address: mcbeker@medipol.edu.tr (Mustafa Caglar Beker)

ration and level of cyclic nucleotide signal transmission in the striatum. Deactivation of PDE10A, in turn, activates cAMP/ protein kinase A (PKA) signaling, which is essential for dopamine neurotransmission in the basal ganglia. Activation of the cAMP/PKA signaling cascade increases phosphorylation of cAMP-response element-binding protein (CREB) and extracellular receptor kinase (ERK)-1/2 [7, 8]. PDE10A inhibition reduced microglial activation in Parkinson's Disease (PD) mouse model [9, 10]. In addition, PDE10A inhibition exerts neuroprotection by reducing apoptosis and pro-inflammatory cytokines/chemokines after traumatic brain injury and focal cerebral ischemia in rodents [11, 12]. Moreover, it is speculated that PDE10A signaling may play an important role in the regulation of circadian rhythm [13, 14].

PDE10A's known and most studied inhibitors so far are MP-10, Compound 1 and TAK-063 [1-[2-fluoro-4-(1H-pyraz ol-1-yl)phenyl]-5-methoxy-3-(1-phenyl-1H-pyrazol-5-yl)pyridazin-4(1H)-one]; the latter being a novel, highly selective inhibitor of PDE10A [15, 16]. Studies demonstrated that Compound 1 and MP-10, used as PDE10A inhibitors, cannot reduce PDE10A protein levels as quickly and effectively as TAK-063 [16]. It has been shown that the half-life of TAK-063 is 3.1 hours and the binding rate of TAK-063 to PDE10A in neurons is over 99% [17, 18]. The experimental studies suggest that PDE10A inhibitors may be used to treat neurodegenerative processes, including PD, Huntington's Disease (HD), cerebral ischemia, traumatic brain injury, and schizophrenia [11, 19].

In the present study, we used 3 mg/ kg TAK-063 to inhibit PDE10A in C57BL/6 mice. Therefore, we identified the protein profile affected by PDE10A inhibition by liquid chromatography with tandem mass spectrometry (LC-MS/MS) mediated proteomic analysis. In addition, the identified proteins were categorized based on their biological activities, molecular functions, and intracellular signal transduction pathways.

Materials and Methods

All procedures including animal treatment were performed in accordance with National Institutes of Health (NIH) guidelines for the care and use of laboratory animals and approved by the Istanbul Medipol University, Animal Research Ethics Committee (Reference number: 10.01.2022-09). Mice were housed in the Istanbul Medipol University animal facility (MEDITAM) in cohorts of 4 or 5 animals per cage and kept under standard animal room conditions (ambient temperature 20±2 °C, 12-12 h light-dark cycle). Investigators were blinded for experimental groups at all experiments and data analysis stages.

Preparation of TAK-063 and experimental groups

TAK-063 (510331, MedKoo Biosciences) was used to inhibit the PDE10A protein expression. TAK-063 was dissolved using tap water containing 1% dimethyl sulfoxide (DMSO).

Twelve adult (8-12 weeks) male C57BL/6 mice were used. Animals were divided into two main groups; vehicle (100 µl tap water containing 1% DMSO) or 3 mg/kg TAK-063 (in 100 µl tap water). Thirty minutes after oral administration of vehicle or 3 mg/kg TAK-063, mice were sacrificed under high-dose anesthesia (4% isoflurane with 30% O_2, remainder N_2O). Then, the brains were removed and frozen on dry ice.

Western blotting

Tissue samples were harvested from the striatum region. Total proteins were extracted from the brain tissue with ice-cold radioimmunoprecipitation assay buffer (RIPA buffer; 89900, Thermo Fisher Scientific, Massachusetts, USA) containing cOmplete™ Protease Inhibitor Cocktail (11697498001, Sigma, USA). After homogenization, samples were centrifugated at 14,000 rpm. The total protein concentration was determined by Qubit 3.0 Fluorometer (Q33216, Invitrogen, Life Technologies Corporation, California, USA). Twenty microgram proteins from the vehicle or TAK-063 groups were size-fractionated using 4-20% Mini-PROTEAN TGX (4561096, Bio-Rad, Life Sciences Research, California, USA) gel electrophoresis. Thereafter, proteins were transferred to a polyvinylidene difluoride membrane (PVDF; 1620174, Bio-Rad, Life Sciences Research) via Trans-Blot Turbo Transfer System (1704155, Bio-Rad, Life Sciences Research). Next, PVDF membranes were blocked in 5% non-fat dry milk (Blotto; sc-2324, Santa Cruz Biotechnology) in 50 mMol Tris-buffered saline (TBS) containing 0.1% Tween (TBS-T; blocking solution) for one hour. Then, the membranes were incubated overnight with monoclonal mouse PDE10A (sc-515023; Santa Cruz Biotechnology) or polyclonal rabbit anti-β-actin (4967, Cell Signaling Technology) antibodies. The next day, membranes were washed three times with TBS-T and treated with appropriate secondary antibodies (31460 or 31430; Thermo Fisher Scientific) at room temperature. After one hour of incubation, membranes were incubated with WesternBright ECL kit (K-12045-D20, BioLegend) and visualized via ChemiDoc MP Imaging System (1708280, Bio-Rad). Thereafter, PDE10A protein abundance was densitometrically calculated by Image J software (National Institute of Health). The relative expression of PDE10 was normalized to β-actin. Western blot analyses were performed for at least three times for each protein.

Sample preparation for liquid chromatography tandem-mass spectrometry (LC-MS/MS) analysis

Sample preparation for LC-MS/MS analysis was performed according to previously published protocols [20, 21]. Briefly, a fifty mM ammonium bicarbonate solution was added to the brain tissue samples for tissue homogenization. Then, the samples were heated up to 95°C in a protein extraction kit (UPX Universal; Expedon, Heidelberg, Germany), incubated (1 h at 4C), and centrifuged at 14,000 G for 10 min. Supernatant concentration was calculated via Qubit 3.0 Fluorometer. To obtain tryptic peptides, Filter Aided Sample Preparation (FASP; ab270519, Abcam) kit was used according to the instructions [22]. Fifty microgram samples were filtered and alkylated with ten mM iodoacetamide. After that, protein samples were treated with mass-spectrometry grade trypsin protease (90057, Thermo Fisher Scientific) enzyme and incubated

at 37°C for 16 h. The next day, samples were centrifuged at 14.000 G for 10 min and lyophilized. Lyophilized peptides were dissolved in 0.1% formic acid (1002642510, Merck) and diluted to 100 ng/µl at the end of the lyophilization process.

LC-MS/MS analysis

LC-MS/MS analysis using ACQUITY UPLC M-Class coupled to a SYNAPT G2-Si high-definition mass spectrometer (Waters) was performed according to previously published protocols with minor modifications [20, 21]. ACQUITY UPLC M-Class Symmetry C18 trap column (180 µm x 20 mm; 186007496, Waters) and the analytic column (ACQUITY UPLC M-Class HSS T3 Column, 100Å, 1.8 µm, 75 µm X 250 mm; 186007474, Waters) were used for the peptide separation [23]. All 50-1900 m/z ions were fragmented in resolution mode without any precursor ion preselection.

Data processing

Progenesis-QI for proteomics software (Waters) was used to identify and quantify the peptides. All proteins were identified by at least 2 unique peptide sequences. Then the expression ratio of identified proteins was calculated and demonstrated as a heatmap. Next, the identified proteins were classified based on their biological activities, molecular functions, and signal transduction pathways using the PANTHER (protein annotation through evolutionary relationship, http://www.pantherdb.org/) program.

Statistical analysis

Statistical analyses were performed with SPSS program version 15, SPSS Inc., Chicago, USA) to determine the differences between groups (Vehicle and TAK-063). Statistical differences between the groups were calculated by conducting the independent samples t-test. Data are expressed as the mean ± standard deviation. Throughout the study, p values < 0.05 were considered significant [13].

Results

Western blotting was performed with brain tissue samples taken from the striatum region to investigate the effect of TAK-063 (3 mg/kg), delivered by oral gavage, on the PDE10A protein expression. Results demonstrated that PDE10A protein abundance in the mice brain significantly diminished by the administration of 3 mg/kg TAK-063 (Figure 1).

The protein profile affected by PDE10A inhibition was demonstrated via LC-MS/MS-based proteomic analyses. We identified 1873 different proteins between the vehicle and TAK-063 groups. Sixty-one proteins significantly ($p<0.05$, independent sample t-test) altered between the groups. TAK-063 treatment significantly decreased 26S proteasome non-ATPase regulatory subunit 2 (PSMD2), Amyloid-like protein 1 (APLP1), Ankyrin repeat domain-containing protein 17 (ANKRD17), Apolipoprotein E (APOE), ATP synthase subunit alpha (ATP5F1A), ATP synthase subunit beta (ATP5F1B), ATP synthase subunit O (ATP5PO), Calcium-binding mitochondrial carrier protein Aralar1

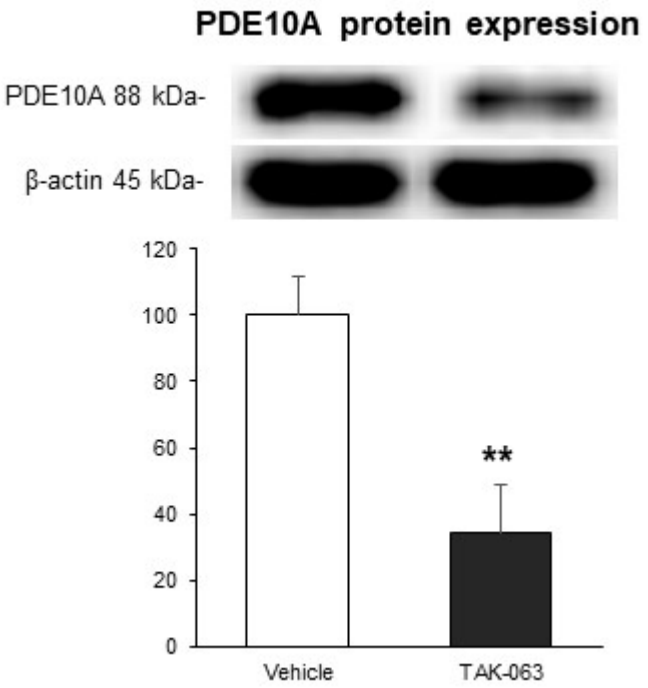

Figure 1. Analysis of PDE10A protein abundance. Orally administered 3 mg/kg TAK-063 significantly reduces PDE10A protein expression. Data was represented as mean ± standard deviation (SD). **$p<0.01$ indicates statistical difference (independent samples t test) according to vehicle treated group.

(SLC25A12), Calcium-binding mitochondrial carrier protein SCaMC-3 (SLC25A23), COP9 signalosome complex subunit 6 (COPS6), Cytochrome c oxidase subunit 6A1 (COX6A1), Dedicator of cytokinesis protein 4 (DOCK4), DNA polymerase zeta catalytic subunit (REV3L), Fibronectin (FN1), Gasdermin-E (GSDME), Hydroxyacylglutathione hydrolase (HAGH), Importin subunit alpha-4 (KPNA3), Mitochondrial 2-oxoglutarate/malate carrier protein (SLC25A11), NADH dehydrogenase [ubiquinone] 1 beta subcomplex subunit 4 (NDUFB4), NADH dehydrogenase [ubiquinone] iron-sulfur protein 4 (NDUFS4), NADPH--cytochrome P450 reductase (POR), Neuronal pentraxin receptor (NPTXR), Neuroplastin (NPTN), Osteopontin (SPP1), Peptidyl-prolyl cis-trans isomerase D (PPID), Potassium-transporting ATPase alpha chain 2 (ATP12A), Proline-rich protein 12 (PRR12), Proteasome subunit alpha type-1 (PSMA1), Ras-related protein Rab-8B (RAB8A), Reticulon (RTN1), Rho-associated protein kinase 2 (ROCK2), Secretory carrier-associated membrane protein (SCAMP1), Separin (ESPL1), Spectrin beta chain (SPTBN4), STE20-like serine/threonine-protein kinase (SLK), Ubiquitin-specific peptidase 9, Y chromosome (USP9Y), and Voltage-dependent anion-selective channel protein 3 (VDAC3) amount with respect to the vehicle treated group (Figure 2).

Moreover, deactivation of PDE10A significantly increased Acyl-CoA-binding protein (DBI), Aldo-keto reductase family 1 member A1 (AKR1A1), Ankyrin-2 (ANK2), Band 4.1-like protein 2 (EPB41L2), Cytosolic acyl

Fold change	Accession number	Symbol	Description
0,74	Q8VDM4	Psmd2	26S proteasome non-ATPase regulatory subunit 2
2,07	P31786	Dbi	Acyl-CoA-binding protein
1,53	Q9JII6	Akr1a1	Aldo-keto reductase family 1 member A1
0,70	Q03157	Aplp1	Amyloid-like protein 1
0,68	E9Q804	Ankrd17	Ankyrin repeat domain-containing protein 17
1,84	S4R2Q9	Ank2	Ankyrin-2
0,67	P08226	Apoe	Apolipoprotein E
0,67	Q03265	Atp5f1a	ATP synthase subunit alpha
0,75	P56480	Atp5f1b	ATP synthase subunit beta
0,74	Q9DB20	Atp5po	ATP synthase subunit O
1,50	Q80UE5	Epb41l2	Band 4.1-like protein 2
0,76	Q8BH59	Slc25a12	Calcium-binding mitochondrial carrier protein Aralar1
0,72	F7BBH5	Slc25a23	Calcium-binding mitochondrial carrier protein SCaMC-3
0,67	D3Z0F5	Cops6	COP9 signalosome complex subunit 6
0,57	Q9DCW5	Cox6a1	Cytochrome c oxidase subunit 6A1
1,75	Q91V12	Acot7	Cytosolic acyl coenzyme A thioester hydrolase
0,72	P59764	Dock4	Dedicator of cytokinesis protein 4
0,60	Q61493	Rev3l	DNA polymerase zeta catalytic subunit
1,81	Q80UW2	Fbxo2	F-box only protein 2
0,40	Q3UHL6	Fn1	Fibronectin
0,60	Q9Z2D3	Gsdme	Gasdermin-E
1,84	P10649	Gstm1	Glutathione S-transferase Mu 1
0,68	Q99KB8	Hagh	Hydroxyacylglutathione hydrolase
0,72	O35344	Kpna3	Importin subunit alpha-4
1,44	Q9Z127	Slc7a5	Large neutral amino acids transporter small subunit 1
1,38	Q99PU5	Acsbg1	Long-chain-fatty-acid--CoA ligase ACSBG1
1,54	Q99LB6	Mat2b	Methionine adenosyltransferase 2 subunit beta
2,75	Q9EQ20	Aldh6a1	Methylmalonate-semialdehyde dehydrogenase
0,73	Q9CR62	Slc25a11	Mitochondrial 2-oxoglutarate/malate carrier protein
1,54	Q9DAT5	Trmu	Mitochondrial tRNA-specific 2-thiouridylase 1
0,75	Q9CQC7	Ndufb4	NADH dehydrogenase [ubiquinone] 1 beta subcomplex subunit 4
0,75	Q9CXZ1	Ndufs4	NADH dehydrogenase [ubiquinone] iron-sulfur protein 4
0,76	Q05DV1	Por	NADPH--cytochrome P450 reductase
0,78	Q99J85	Nptxr	Neuronal pentraxin receptor
0,74	P97300	Nptn	Neuroplastin
1,47	Q5SSP3	Slc1a4	Neutral amino acid transporter A
1,38	P29758	Oat	Ornithine aminotransferase
0,23	P10923	Spp1	Osteopontin
0,75	Q9CR16	Ppid	Peptidyl-prolyl cis-trans isomerase D
1,60	Q6GT24	Prdx6	Peroxiredoxin
1,33	Q8VIN1	Pbp2	Phosphatidylethanolamine-binding protein 1
0,74	Q9Z1W8	Atp12a	Potassium-transporting ATPase alpha chain 2
0,65	E9PYL2	Prr12	Proline-rich protein 12
0,74	Q9R1P4	Psma1	Proteasome subunit alpha type-1
3,05	P50114	S100b	Protein S100-B
1,72	Q9Z2Y8	Plpbp	Pyridoxal phosphate homeostasis protein
1,98	Q60790	Rasa3	Ras GTPase-activating protein 3
1,32	J3QQ18	Syngap1	Ras/Rap GTPase-activating protein SynGAP
0,75	P55258	Rab8a	Ras-related protein Rab-8B
0,76	A3QM89	Rtn1	Reticulon
0,76	P70336	Rock2	Rho-associated protein kinase 2
0,73	Q3TSA8	Scamp1	Secretory carrier-associated membrane protein
0,73	P60330	Espl1	Separin
1,50	Q8R3F9	Tut1	Speckle targeted PIP5K1A-regulated poly(A) polymerase
0,70	Q91ZE6	Sptbn4	Spectrin beta chain
0,65	O54988	Slk	STE20-like serine/threonine-protein kinase
1,40	P97797	Sirpa	Tyrosine-protein phosphatase non-receptor type substrate 1
0,77	F8VPU6	Usp9y	Ubiquitin-specific peptidase 9, Y chromosome
0,72	J3QMG3	Vdac3	Voltage-dependent anion-selective channel protein 3
1,37	F6VYE2	Zmym4	Zinc finger MYM-type protein 4
1,27	B2RRF6	Znf518a	Zinc finger protein 518A

Figure 2. Heatmap visualization of the PDE10A related proteins. The protein profile affected by 3 mg/kg TAK-063 was determined by liquid chromatography-mass spectrometry/mass spectrometry (LC-MS/MS) mediated proteomic analyzes.

coenzyme A thioester hydrolase (ACOT7), F-box only protein 2 (FBXO2), Glutathione S-transferase Mu 1 (GSTM1), Large neutral amino acids transporter small subunit 1 (SLC7A5), Long-chain-fatty-acid--CoA ligase ACSBG1 (ACSBG1), Methionine adenosyltransferase 2 subunit beta (MAT2B), Methylmalonate-semialdehyde dehydrogenase (ALDH6A1), Mitochondrial tRNA-specific 2-thiouridylase 1 (TRMU), Neutral amino acid transporter A (SLC1A4), Ornithine aminotransferase (OAT), Peroxiredoxin (PRDX6), Phosphatidylethanolamine-binding protein 1 (PBP2), Protein S100-B (S100B), Pyridoxal phosphate homeostasis protein (PLPBP), Ras GTPase-activating protein 3 (RASA3), Ras/Rap GTPase-activating protein SynGAP (SYNGAP1), Speckle targeted PIP5K1A-regulated poly(A) polymerase (TUT1), Tyrosine-protein phosphatase non-receptor type substrate 1 (SIRPA), Zinc finger MYM-type protein 4 (ZMYM4), and Zinc finger protein 518A (ZNF518A) amount (Figure 2).

Identified proteins were classified using the PANTHER (protein annotation through evolutionary relationship, http://www.pantherdb.org/) program. The identified proteins were predicted to belong to 5 protein classes: metabolite interconversion enzyme (10 proteins), protein modifying enzyme (5 proteins), protein-binding activity modulator (4 proteins), transfer/ carrier protein (2 proteins), and transporter (8 proteins) (Figure 3A). Molecular function-related classification showed that 8 binding, 15 catalytic activity, 1 molecular function regulator, and 7 transporter activity proteins were identified (Figure 3B). Then, the identified proteins were mapped to seven important cell signaling pathways (Figure 3C) including ATP synthesis, FGF signaling, EGF receptor signaling HD, PD, pyrimidine metabolism, and ubiquitin-proteasome pathway.

Discussion

Twenty-one different genes encode eleven various members of the PDE family, leading to the production of more than 100 different enzymes [24]. PDE10A has become a prominent therapeutic target in recent years because it is highly

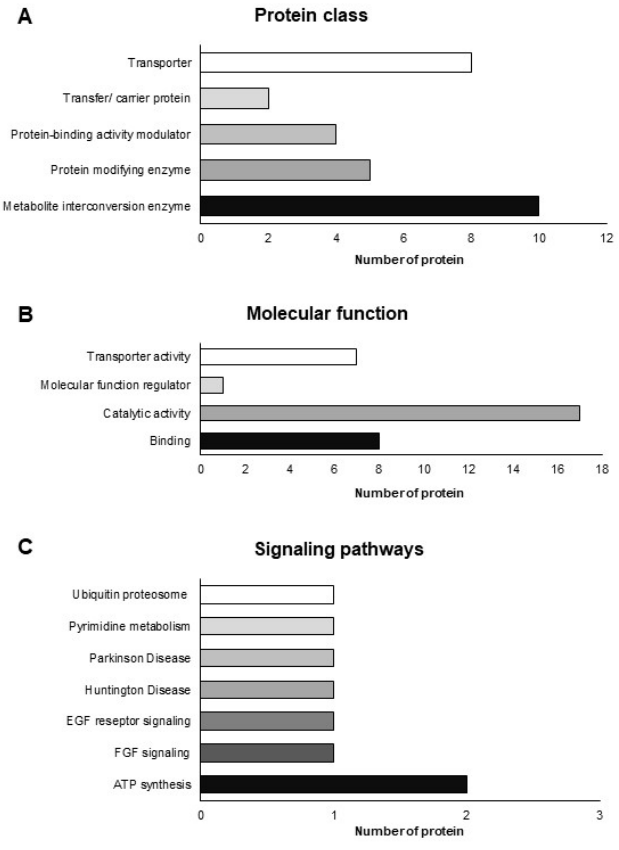

Figure 3. Classification of PDE10A related proteins. PDE10A related proteins were classified with respect to (A) protein class, (B) molecular function, and (C) signal transduction pathway by the PANTHER (protein annotation through evolutionary relationship; http://www.pantherdb.org/) program.

available and scattered through the mammalian striatum, which is one of the principal components of the basal ganglia. PDE10A hydrolyzes and controls the level of cGMP and cAMP, which are essential in regulating intracellular signal transduction pathways [25]. Recent studies indicated that PDE10A plays pivotal role in modulating striatal neuronal activity in motor and cognitive processes [26, 27]. Due to its modulatory functions in the CNS, it is speculated that PDE10A may be an essential target in the treatment of neurodegenerative diseases.

TAK-063 is the most studied and well-known inhibitor for PDE10A. We previously demonstrated that oral delivery of 0.3 mg/kg and 3 mg/kg TAK-063 reduced PDE10A protein abundance 25% and %51, respectively [11]. It has been shown that TAK-063 does not affect plasma prolactin and glucose levels up to 3 mg/kg [28]. In the current study, we used high (3 mg/kg) dose of TAK-063 to inhibit PDE10A activity effectively. In accordance with the literature, oral delivery of high dose TAK-063 significantly reduced PDE10A protein abundance in mice striatum compared to the vehicle-treated mice.

Proteomics is an essential member of the omics technologies (genomics, transcriptomics, proteomics, and metabolomics). It serves as an emerging tool for the identification and quantification of the proteome of tissues and cells. Characterization of the proteome is crucial for diagnosing, prognosis, and monitoring of the disease developments [29]. Moreover, it is essential for the drug development studies. In the present study, we demonstrated that the protein profile affected by the TAK-063 mediated PDE10A inhibition under physiological conditions. Because of this, we performed LC-MS/MS based proteomic analysis. Chemical deactivation of PDE10A significantly altered 61 different protein expressions in the mice striatum. According to the proteomic analysis PSMD2, APLP1, ANKRD17, APOE, ATP5F1A, ATP5F1B, ATP5PO, SLC25A12, SLC25A23, COPS6, COX6A1, DOCK4, REV3L, FN1, GSDME, HAGH, KPNA3, SLC25A11, NDUFB4, NDUFS4, POR, NPTXR, NPTN, SPP1, PPID, ATP12A, PRR12, PSMA1, RAB8A, RTN1, ROCK2, SCAMP1, ESPL1, SPTBN4, SLK, USP9Y, and VDAC3 protein abundance decreased by PDE10A inhibition. However, protein abundance of DBI, AKR1A1, ANK2, EPB41L2, ACOT7, FBXO2, GSTM1, SLC7A5, ACSBG1, MAT2B, ALDH6A1, TRMU, SLC1A4, OAT, PRDX6, PBP2, S100B, PLPBP, RASA3, SYNGAP1, TUT1, SIRPA, ZMYM4, and ZNF518A increased by deactivation of PDE10A.

It is well known that TAK-063 improves behavioral deficits in a mouse model of HD, however decreases disseminated neuronal injury after brain injury, and regulates pro- and anti-inflammatory cytokines and chemokines in rodents [11, 12, 30]. Moreover, it is suggested that TAK-063 has therapeutic potential for basal ganglia disorders [24]. We proposed that the identified proteins in the current study could potentially increase the effectiveness of TAK-063. In this way, we speculated that TAK-063 could be used more effectively in the treatment of neurodegenerative diseases.

Sixty-one differentially expressed proteins were classified extensively into several categories via PANTHER analysis. The classification of the protein class includes metabolite interconversion enzyme, transporter, protein modifying enzyme, protein-binding activity modulator, and transfer/ carrier protein. The identified proteins are suggested to belong to 4 different molecular functions as catalytic activity, binding, transporter activity, and molecular function regulator. In addition, the intracellular signal transduction pathway analysis demonstrated that PDE10A-related proteins have essential roles in ATP synthesis, FDF signaling, EGF receptor signaling, pyrimidine metabolism, and ubiquitin-proteasome signal transduction pathways. Furthermore, the identified proteins are involved in the mechanism of neurodegenerative diseases such as HD and PD.

Altogether, the proteomics profiles indicate that ATP synthesis is the most affected signal transduction pathway due to PDE10A inhibition. Although the effects of PDE10A on energy metabolism have been demonstrated in previous studies, its mechanism has not yet been fully understood [31, 32]. A recent study using transgenic HD mice revealed that the protein and mRNA expression of PDE10A significantly reduced in the striatum before the onset of motor symptoms [33]. Furthermore, in mice with HD pathology, chemical deactivation of PDE10A decreased striatal and cortical cell death and microglial activation [34]. In a mouse PD model, deactivation of PDE10A has been shown to increase neuronal survival and decrease microglial activation via the cAMP/ protein kinase A (PKA) signal transduction pathway [35].

Conclusion

In conclusion, the chemical deactivation of PDE10A using 3 mg/kg TAK-063 directly or indirectly affects the abundance of 61 different proteins in the mice striatum under physiological conditions. It is suggested that the identified proteins might enhance the activity and effectiveness of TAK-063. Moreover, these proteins might be essential in PDE10A-related signal transduction pathways.

Funding

This study was supported by TUBITAK (The Scientific and Technological Research Council of Turkey/ 218S453; MCB) and Turkish Academy of Sciences (TUBA; EK).

Conflicts of interest

The authors declare that they have no conflict of interest.

Ethics approval

Experiments were performed in accordance to National Institutes of Health (NIH) guidelines for the care and use of laboratory animals and approved by Istanbul Medipol University, Animal Research Ethics Committee (Reference number: 10.01.2022-09).

References

1. Conti M, Beavo J. Biochemistry and physiology of cyclic nucleotide phosphodiesterases: essential components in cyclic nucleotide signaling. Annual review of biochemistry. 2007;76:481-511.

2. Xu Y, Zhang HT, O'Donnell JM. Phosphodiesterases in the central nervous system: implications in mood and cognitive disorders. Handbook of experimental pharmacology. 2011(204):447-85.
3. Titus DJ, Oliva AA, Wilson NM, Atkins CM. Phosphodiesterase inhibitors as therapeutics for traumatic brain injury. Curr Pharm Des. 2015;21(3):332-42.
4. Muller-Deubert S, Ege C, Krug M, et al. Phosphodiesterase 10A Is a Mediator of Osteogenic Differentiation and Mechanotransduction in Bone Marrow-Derived Mesenchymal Stromal Cells. Stem Cells Int. 2020;2020:7865484.
5. Barnes TD, Kubota Y, Hu D, et al. Activity of striatal neurons reflects dynamic encoding and recoding of procedural memories. Nature. 2005;437(7062):1158-61.
6. Yin HH, Mulcare SP, Hilario MR, et al. Dynamic reorganization of striatal circuits during the acquisition and consolidation of a skill. Nature neuroscience. 2009;12(3):333-41.
7. Giralt A, Saavedra A, Carreton O, et al. PDE10 inhibition increases GluA1 and CREB phosphorylation and improves spatial and recognition memories in a Huntington's disease mouse model. Hippocampus. 2013;23(8):684-95.
8. Kong T, Liu M, Ji B, et al. Role of the Extracellular Signal-Regulated Kinase 1/2 Signaling Pathway in Ischemia-Reperfusion Injury. Front Physiol. 2019;10:1038.
9. Kim DY, Park JS, Leem YH, et al. The Potent PDE10A Inhibitor MP-10 (PF-2545920) Suppresses Microglial Activation in LPS-Induced Neuroinflammation and MPTP-Induced Parkinson's Disease Mouse Models. J Neuroimmune Pharmacol. 2021;16(2):470-82.
10. Yamazaki Y, Kawano Y. Inhibitory effects of herbal alkaloids on the tumor necrosis factor-alpha and nitric oxide production in lipopolysaccharide-stimulated RAW264 macrophages. Chem Pharm Bull (Tokyo). 2011;59(3):388-91.
11. Beker MC, Caglayan AB, Altunay S, et al. Phosphodiesterase 10A Is a Critical Target for Neuroprotection in a Mouse Model of Ischemic Stroke. Mol Neurobiol. 2022;59(1):574-89.
12. Huang J, Tang D, Cao Y, et al. Inhibition of PDE10A-Rescued TBI-Induced Neuroinflammation and Apoptosis through the cAMP/PKA/NLRP3 Pathway. Evid Based Complement Alternat Med. 2022;2022:3311250.
13. Beker MC, Kilic E. The role of circadian rhythm in the regulation of cellular protein profiles in the brain. Turk J Med Sci. 2020.
14. Wolloscheck T, Spiwoks-Becker I, Rickes O, et al. Phosphodiesterase10A: abundance and circadian regulation in the retina and photoreceptor of the rat. Brain Res. 2011;1376:42-50.
15. Kehler J, Nielsen J. PDE10A inhibitors: novel therapeutic drugs for schizophrenia. Current pharmaceutical design. 2011;17(2):137-50.
16. Suzuki K, Harada A, Suzuki H, et al. TAK-063, a PDE10A Inhibitor with Balanced Activation of Direct and Indirect Pathways, Provides Potent Antipsychotic-Like Effects in Multiple Paradigms. Neuropsychopharmacology : official publication of the American College of Neuropsychopharmacology. 2016;41(9):2252-62.
17. Tohyama K, Sudo M, Morohashi A, et al. Pre-clinical Characterization of Absorption, Distribution, Metabolism and Excretion Properties of TAK-063. Basic & clinical pharmacology & toxicology. 2018;122(6):577-87.
18. Takano A, Stenkrona P, Stepanov V, et al. A human [(11)C]T-773 PET study of PDE10A binding after oral administration of TAK-063, a PDE10A inhibitor. Neuroimage. 2016;141:10-7.
19. Zagorska A, Partyka A, Bucki A, et al. Phosphodiesterase 10 Inhibitors - Novel Perspectives for Psychiatric and Neurodegenerative Drug Discovery. Curr Med Chem. 2018;25(29):3455-81.
20. Yalcin E, Beker MC, Turkseven S, et al. Evidence that melatonin downregulates Nedd4-1 E3 ligase and its role in cellular survival. Toxicology and applied pharmacology. 2019;379:114686..
21. Beker MC, Caglayan B, Yalcin E, et al. Time-of-Day Dependent Neuronal Injury After Ischemic Stroke: Implication of Circadian Clock Transcriptional Factor Bmal1 and Survival Kinase AKT. Molecular neurobiology. 2018;55(3):2565-76.
22. Wisniewski JR, Zougman A, Nagaraj N, Mann M. Universal sample preparation method for proteome analysis. Nature methods. 2009;6(5):359-62.
23. Acioglu C, Mirabelli E, Baykal AT, et al. Toll like receptor 9 antagonism modulates spinal cord neuronal function and survival: Direct versus astrocyte-mediated mechanisms. Brain, behavior, and immunity. 2016;56:310-24.
24. Suzuki K, Kimura H. TAK-063, a novel PDE10A inhibitor with balanced activation of direct and indirect pathways, provides a unique opportunity for the treatment of schizophrenia. CNS Neurosci Ther. 2018;24(7):604-14.
25. Fujishige K, Kotera J, Michibata H, et al. Cloning and characterization of a novel human phosphodiesterase that hydrolyzes both cAMP and cGMP (PDE10A). J Biol Chem. 1999;274(26):18438-45.
26. Birjandi SZ, Abduljawad N, Nair S, et al. Phosphodiesterase 10A Inhibition Leads to Brain Region-Specific Recovery Based on Stroke Type. Transl Stroke Res. 2021;12(2):303-15.
27. Russwurm C, Koesling D, Russwurm M. Phosphodiesterase 10A Is Tethered to a Synaptic Signaling Complex in Striatum. J Biol Chem. 2015;290(19):11936-47.
28. Suzuki K, Harada A, Shiraishi E, Kimura H. In vivo pharmacological characterization of TAK-063, a potent and selective phosphodiesterase 10A inhibitor with antipsychotic-like activity in rodents. J Pharmacol Exp Ther. 2015;352(3):471-9.
29. Aslam B, Basit M, Nisar MA, et al. Proteomics: Technologies and Their Applications. J Chromatogr Sci. 2017;55(2):182-96.
30. Harada A, Suzuki K, Kimura H. TAK-063, a Novel Phosphodiesterase 10A Inhibitor, Protects from Striatal Neurodegeneration and Ameliorates Behavioral Deficits in the R6/2 Mouse Model of Huntington's Disease. J Pharmacol Exp Ther. 2017;360(1):75-83.
31. Hankir MK, Kranz M, Gnad T, et al. A novel thermoregulatory role for PDE10A in mouse and human adipocytes. EMBO Mol Med. 2016;8(7):796-812.
32. Siuciak JA, McCarthy SA, Chapin DS, et al. Genetic deletion of the striatum-enriched phosphodiesterase PDE10A: evidence for altered striatal function. Neuropharmacology. 2006;51(2):374-85.
33. Hebb AL, Robertson HA, Denovan-Wright EM. Striatal phosphodiesterase mRNA and protein levels are reduced in Huntington's disease transgenic mice prior to the onset of motor symptoms. Neuroscience. 2004;123(4):967-81.
34. Giampa C, Laurenti D, Anzilotti S, et al. Inhibition of the striatal specific phosphodiesterase PDE10A ameliorates striatal and cortical pathology in R6/2 mouse model of Huntington's disease. PloS one. 2010;5(10):e13417.
35. Lee YY, Park JS, Leem YH, et al. The phosphodiesterase 10 inhibitor papaverine exerts anti-inflammatory and neuroprotective effects via the PKA signaling pathway in neuroinflammation and Parkinson's disease mouse models. Journal of neuroinflammation. 2019;16(1):246.